FRAGMENTATION ANALYSIS OF DRIPLINE NUCLEI IN VIEW OF PROTON RADIOACTIVITY

A Thesis submitted in partial fulfillment of the requirements for the award of degree of

Masters of Science

In

Physics

Submitted by

Rupinder Kaur

Roll No. 301404023

Under the supervision of

Dr. MANOJ K. SHARMA

Professor and Head

SPMS

Thapar University, Patiala

School of Physics and Material Science,

Thapar University,

(Formerly Thapar Institute of Engineering and Technology)

Patiala-147004, INDIA

July-2016

Dedicated

to

God and my loving family.

CERTIFICATE

I hereby certify that the work which has been presented in this thesis entitled **"Fragmentation analysis of dripline nuclei in view of proton radioactivity"** submitted for partial fulfillment of the requirements for the award of degree **of Master of Science in Physics** at **Thapar University, Patiala**, is an authentic record of my own work carried out under the supervision of **Dr. Manoj K. Sharma, Professor and Head, SPMS** and refers other researcher's work which are duly listed in reference section.

The matter embodied in this thesis has not been submitted for the award of any other degree of this or any other university.

Rupinder

Date: 15-July-2016 (Rupinder kaur)

This is to certify that the above statement made by the candidate is correct and true to best of my knowledge.

MSharma

Dr. Manoj K. Sharma

Professor and head,

SPMS

Thapar University,

Patiala

Counter signed by:

DBhatia

Dr. S.S. Bhatia

Dean of Academic Affairs,

Thapar University,

Patiala- 147004.

ACNOWLEDGEMENT

I would first like to thank god because without his blessings, I wouldn't have anything to be thankful for and then my family for the encouragement and care. I express my deep sense of gratitude to **Dr. MANOJ K. SHARMA** for his suggestions, planning and supervising this work that benefitted me in completion and success of this study. I sincerely thank him for introducing me to nuclear physics. I will always be grateful for having the opportunity to work under his guidance.

My special thanks goes to **Miss Kanishka Sharma** for her advice, guidance and giving endless help to finish this work. I am very thankful for having such a good advisor like her. Without her guidance and help, this dissertation would not have been possible. Thanks are also due to all the research scholars of nuclear physics lab for their timely help.

Rupinder

Date: 15th July 2016

Rupinder Kaur

Contents:

List of Figures/Tables

Table1.2: Experimental logarithm of half lives, Q_P values and ℓ values of proton decay from different deformed proton emitters.

Table 3.1: Spherical proton emitters measured so far with experimental ℓ and Q values and calculated values of $P_{0,}P$, half lives (calculated with old and new binding energies).

Table 3.2: Deformed proton emitters measured so far with experimental ℓ and Q values and calculated values of $P_{0,}P$, half lives (calculated with old and new binding energies).

ABSTRACT

Investigation of nuclear properties, structure of exotic nuclei, exploration of unknown areas of periodic table and mapping the proton drip-line has been prominent area of research in nuclear physics. The discovery of radioactivity has played a crucial role in achieving these research goals. α, β, γ and cluster decays are well known radioactive decay paths observed during last century. Here in present work we intend to emphasize on relatively less explored radioactive decay called as proton decay. Emission of proton from ground state of parent nuclei has been observed experimentally in 1980, at GSI. Since then, with the experimental developments more than 25 cases of proton radioactivity have been identified. These proton emitters lie beyond the limit of nuclear stability on the chart of nuclides i.e. proton drip-line. The purpose of present work is to explore the role of new binding energies and their comparison with earlier data on binding energies besides addressing the possible role of deformation effects governed within quantum mechanical fragmentation approach. The role of shell effects is also explored and most probable proton decays can be predicted. The effect of orbital angular momentum on half lives and fragmentation profile of various proton emitters is also addresed.

Half life estimations for the ground state (spherical as well as deformed) proton emitters are done by using theoretical approach known as preformed cluster decay model (PCM) which is on based on quantum mechanical fragmentation theory (QMFT).

The dissertation consists of three chapters:

Chapter 1:

Chapter-1 gives an overview of the various ground state decays, phenomenon of proton radioactivity, various spherical and deformed proton emitters, In addition to this, the associated features such as nuclear shapes, role of binding energies etc are also discussed in this chapter.

Chapter 2:

Chapter-2 includes brief description of Preformed Cluster Decay Model (PCM). It carries the brief description of various potentials used in methodology. The other related parameters

such as preformation factor; barrier penetrability, etc are outlined. The use of deformations in PCM domain is also discussed.

Chapter 3:

Chapter-3 consists of the PCM based calculations for various cases of spherical and deformed proton emitters. Various results regarding the study of proton decay are discussed and related conclusions are drawn for better description of related concepts.

Chapter 1

Literature Review

1.1 Introduction

Nuclear physics comprises of the study of atomic nuclei, their structure, nuclear reactions, forces between nucleons and nuclei and related decay mechanism etc. It overlaps with many other fields as well, since nuclei are involved in wide variety of pure and applied research. It is also the pillar of astrophysics where it helps to understand the origin of the universe. As stellar evolution and nucleo-synthesis are related to low energy nuclear reactions, henceforth the subject is not only of interest to nuclear physicists but also to the astrophysicists. Nuclear properties have many other applications such as in nuclear medicines, nuclear energy etc for which proper knowledge of nuclear physics is essential.

The research on the structure of atomic nucleus began just after the discovery of radioactivity. Radioactivity began with two accidental discoveries. On Nov. 8^{th}, 1895, Professor Wilhelm Rontgen was doing experiment with discharge tube, when the luminescent screen which was accidently left on a table was scintillating. This led to the discovery of X-rays. On March 1896, Henri Becquerel was checking if the radiations from the phosphorescent material are X-rays or not, however, his experiment did not work because of the cloudy weather but he discovered that Uranium salt emits radiations that blacken the photographic plates. He named these rays as "Becquerel Rays". He lost interest in the subject within following six months. But In 1899, Ernest Rutherford followed the concept and did series of experiments leading to the discovery of nucleus (1911) and alpha, beta radiations. Earlier in 1900, P. Villard found additional penetrating radiations named gamma rays. Marie Curie gave the characteristics of radioactivity through her experiments by isolating different elements produced in the decay of Uranium.

The phenomenon of radioactivity is responsible for the understanding of the structure of the atom and nucleus as well. In 1911, Rutherford figured out the inside view of atom by bombarding atoms with alpha rays and studying alpha particles impact on fluorescent screen. With the results of his experimental work, Rutherford came up with the conclusion that the nucleus is made up of positively charged particles. Eventually, by the contribution of other scientists, structure and many other properties of constituents of the atom were explored.

Here in present work, we intend to work on nuclear structure, decay mechanisms and other quantities like half lives, Q-values etc. of the nucleus are to be evaluated in the present work.

Stability of nucleus is due to the balance of two forces; first is the strong nuclear force which is short range but attractive and second is Coulomb force which is long range and repulsive. Black squares in figure 1.1 represent the list of stable nuclei. At low masses, the line of stability lies close to N = Z line, but beyond A = 40, due to increasing influence of Coulomb repulsion this line shift towards the neutron-rich side. There are very few stable nuclides that lie above ^{208}Pb because short range attractive nuclear forces cannot overcome the long range repulsive Coulomb forces. In context of decay mode, nuclei which are close to the valley of stability generally decay by β emission. They tend to change the N/Z ratio to lie closer to line of stability by emitting an e^- or e^+, less bound nucleons are therefore emitted. β^+ decay is favored decay mode in proton-rich side and β^- decay is favored in neutron-rich side of the valley of stability. This is because nuclei lying away from stability have comparatively higher energy for β decay to occur. The decay occurs quickly leading to decrease in half lifetime of these nuclei. Eventually, the energy available for decay is so large that β-delayed particle emission can occur. In β delayed particle emission, initial nucleus β-decays to an excited state of daughter nucleus which then de-excites by proton, alpha or neutron emission.

In high mass nuclei on proton-rich side of stability line, Coulomb repulsion become more important as Coulomb energy increases faster (αZ^2) than nuclear volume energy (αA). This leads to α emission, which gets emitted to lower the atomic number of unstable nucleus and make it stable. So, α decay becomes dominant decay mode for proton-rich nuclei with Z>82. However, ground state proton decay becomes energetically possible for nuclei past the proton drip-line. Proton emission is generally seen in nuclei beyond the proton drip-line. These ground state proton emitters beyond the proton drip-lines are resonances in which even the low lying states are in continuum i.e. they are unbound to proton decay. As one goes further away from drip-line, proton decay not only competes with α and β emissions but starts dominating these decays. It competes with α and β decays at higher and lower Z respectively. The exploration of exotic nuclei far from line of stability led to the discovery of proton radioactivity. The proton and neutron drip-lines are the lines beyond which nuclei are unstable and unbound with respect to emission of a single nucleon, a neutron for neutron-rich side and proton for proton-rich side. These drip-lines represent the nuclear stability limit. The neutron dripline lies away from the β stability line in comparison to proton dripline because of the presence of Coulomb repulsion in proton-rich nuclei due to which binding energy of

nuclei decreases and are more unstable than their corresponding neutron rich counterparts. As one goes beyond these lines, the nuclear half life time decreases rapidly.

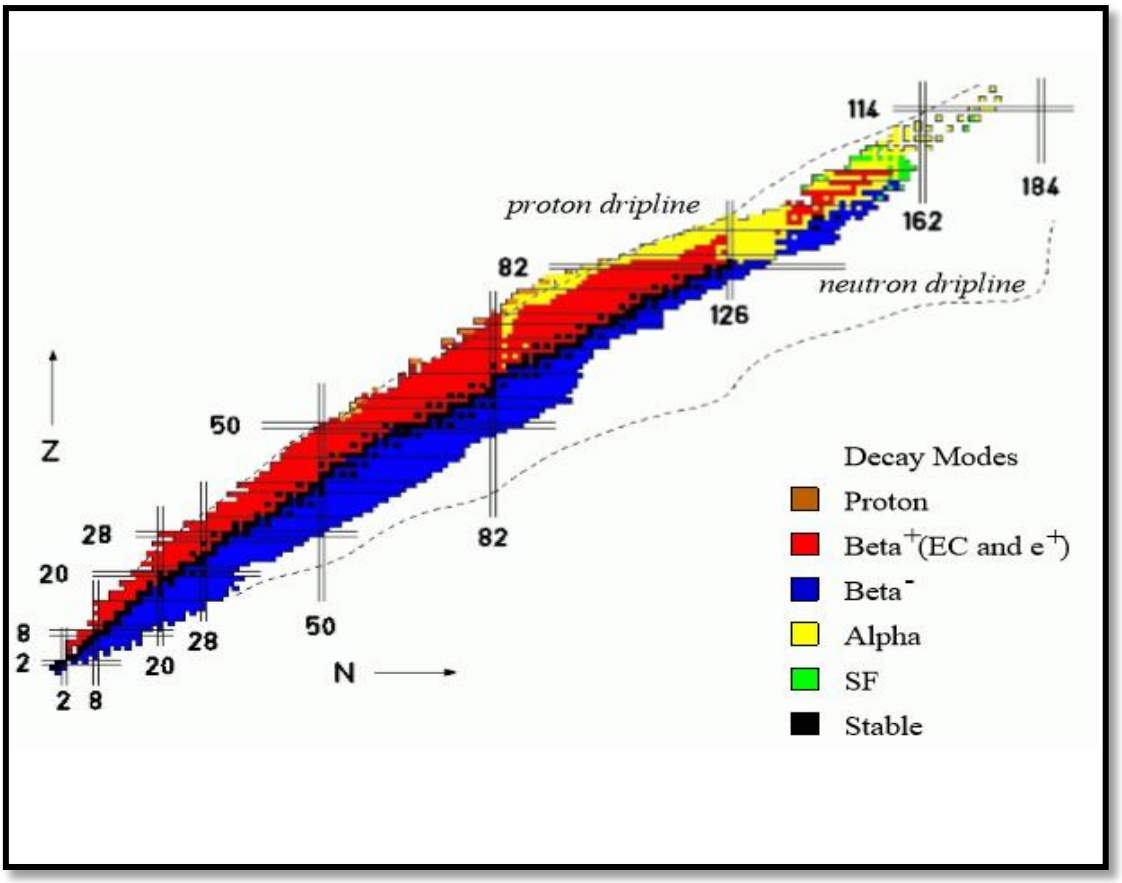

Figure 1.1: *Chart of nuclides, the central black line represents stable nuclei. Dotted lines show the proton and neutron drip-lines[1].*

1.2 Types of decay:

There are two types of decays in context of their energy level from which parent nucleus decays, they are ground state decays and excited state decays. Ground state decays are radioactive decays in which parent nucleus is already in the ground state. The parent nucleus being unstable decays spontaneously. The temperature of decay products and the parent nuclei is zero and angular momentum is nearly zero or having a very small value in these types of decays. The compound nucleus is not formed in ground state decay mechanisms, whereas in excited state decays there is the formation of composite system, the excitation

energy and temperature of the reaction partners, composite system and decay products are non zero and are generally accompanied by significantly large ℓ values. We have confined our study to ground state radioactive decays only which include the following types of radioactive emissions:

1.2.1 Types of ground state emissions:

Initially, radioactive emissions were considered to be of three types: alpha, beta and gamma ray emissions. After 1980's, besides these three types of emissions, some nuclear decays have also been discovered in which a proton or clusters heavier than alpha particle are emitted. These ground state decays include proton decay, cluster decay and heavy particle decay, etc.

Alpha (α), beta (β) and gamma (γ) decay:

Alpha decay is explained by quantum mechanical tunneling through the potential barrier (first application of quantum mechanics to nuclear physics) leading from parent nucleus to the two emitted fragments which have to tunnel through the potential barrier to get emitted. The two fragments emitted are an alpha particle (helium atom) and a daughter nucleus. Before the charged particle accelerators were invented, alpha decay played major role in nuclear physics research. Example of alpha decay [2] may be written as

$$^{209}_{83}\mathrm{Bi} \longrightarrow {}^{205}_{81}\mathrm{Tl} + {}^{4}_{2}\mathrm{He}$$

Q-value of above reaction is 3.137 MeV and is positive for alpha decay to occur spontaneously. Alpha decay energies increase with increase of the atomic number of parent nuclei but energy is not too high (higher than Coulomb barrier) for the reverse reaction to occur.

Alpha decay is the dominant decay process for heavy elements. Elements with A>150 and Z >82 are thermodynamically unstable in case of alpha emission (as Q_α is +ve for them). The energies of α-particles which are emitted can range from 1.8 MeV (^{144}Nd) to 11.6 MeV (^{212}Po) with the half-life of α in ^{144}Nd decay being 10^{29} times as long as in that of ^{212}Po. The released energy is very large if the daughter nucleus is doubly magic. β-particle emission, which is of two types: β^--emission in which electron is emitted and another is β^+-emission in which positron is emitted. γ-emission is the one in which γ rays are emitted. Other possible

decays are cluster radioactivity, heavy particle radioactivity and proton radioactivity which are explained ahead.

Cluster radioactivity:

Cluster radioactivity refers to the spontaneous emission of fragments heavier than alpha particle i.e. having Z lying between Z>2 and lighter than fission fragments. It was first predicted theoretically by Sandulescu, Poenaru and Greiner in 1980 [3] and experimentally observed by Rose and Jones [4] in 1984 for ^{14}C emission from ^{223}Ra. Light clusters ranging from ^{14}C to ^{34}Si are observed experimentally from ^{221} Fr to ^{242} Cm respectively and search for other possible decays is still going on. Theoretically, cluster emitters are nuclei with Z>40 and having positive Q value but practically, it depends on available techniques which need large branching ratio relative to alpha decay. The observed branching ratio relative to α-decay varies from 5×10^{-17} (^{238}Pu→^{32}Si + ^{206}Dy) to 4.1×10^{-9} (^{223}Ra→^{14}C + ^{209}Pb) which is very low therefore the cluster radioactivity is an infrequent process. The energy released as Q-value in the decay, is completely emitted as the kinetic energy of the two fragments due to which cluster radioactivity is a cold nuclear process. The values for half-lives associated with this process are very large and vary in a wide range from $10^{11}$to 10^{26}sec.

The shell effects as well as deformations and orientations also generally affect cluster decay process. For example the role of higher multipole deformations (β_{3i}, β_{4i}, i=1, 2) is crucial for the decay of ^{14} C clusters, on the other hand, quadrupole deformations β_{2i} alone can be utilized to explain other cluster decays [5]. It is observed that ^{14}C radioactivity is somewhat different than other cluster decay processes as the mechanism of higher order deformations is essential to address its dynamics.

Cluster radioactivity has been studied using preformed cluster model (PCM) [5] and by the fission models for example Analytic Super-Asymmetric Fission Model (ASAFM) [6] based on quantum mechanical fragmentation theory [7-9]. Both these models are based on Gamow's theory of barrier penetration. Cluster radioactivity covers two regions in terms of mass of parent nuclei named Pb-radioactivity and Sn-radioactivity.

Pb radioactivity:

In heavy mass region, the most likely mode of cluster radioactivity is Pb radioactivity. In Pb radioactivity, daughter nucleus for the cluster decay is always doubly magic nucleus ^{208}Pb or its neighboring nucleus and the emitted clusters are generally seen to be ^{14}C, ^{18,20}O, ^{23}F,

^{24,26}Ne, ^{28,30}Mg and ^{34}Si etc. Hence, one may assume that the shell structure of daughter nucleus or the Q-value plays a very essential role in the cluster decay phenomenon.

Sn radioactivity:

In the medium mass region, most likely mode of cluster radioactivity is Sn-radioactivity in which parent nuclei generally emits α-like nuclei such as ^{12}C, ^{16}O, ^{20}Ne and^{28}Si and daughter nucleus is around doubly magic ^{100}Sn (Z=50; proton magic number). It was first predicted by Poenaru in 1993 and is based on analytical super asymmetric fission model (ASAFM) [9]. In 1995, Gupta et al. studied the same work using PCM stressing the importance of shell effects. The parent nuclei were from Xenon (Z_P = 54) up to Gadolinium (Z_P =64) (i.e from trans tin region) [11]. In addition to ^{100}Sn radioactivity, there also exists ^{132}Sn radioactivity in which the daughter is always equal to or around doubly magic nucleus ^{132}Sn (N=82; neutron magic number). This kind of radioactivity was also studied by using PCM in 1996 [11].

Heavy particle radioactivity:

Heavy Particle Radioactivity (HPR) is the process in which parent nucleus emits fragment having atomic number Z≥28 but lesser than fission fragments. According to Poenaru et al. [13], heavy-particle radioactivity (HPR) allow the emission of particles with Z > 28 from parents with Z > 110 and daughter around ^{208}Pb, this study revealed that there is probability of observing regions in the super-heavy systems in which the emission of HPR fragment looks possible and calls for experimental verification in near future.

Spontaneous fission (SF):

Heavier elements being unstable split into two nearly equal fragments due to small binding energy strength and liberate a large amount of energy. This phenomenon is called spontaneous fission. This was predicted in 1939 by Bohr and Wheeler [14] on the basis of liquid drop model. In 1940, Flerov et al. [15] observed this phenomenon using ^{238}U nucleus. Spontaneous fission processes are very rare in nature. The reason for SF to occur is that in order to split a nucleus into two parts, the nucleus must first undergo a deformation of its shape into an ellipsoidal shape and then a ‘neck' develops in the middle before it finally breaks into two nuclei. Generally, a nucleus having $Z^2/A > 18$ undergoes spontaneous fission and it is observed mainly in nuclei beyond ^{232}Th, although with a very small probability. Note that in fission, the half lives of both fragments (light and heavy) are measured simultaneously, in contrast to the exotic cluster-decay process where half-lives of only lighter

fragments are measured. The mean lifetime of the above process is about 10^{17} years compared to the mean lifetime for α-decay from the same nuclide which is about 10^{11} years [16]. SF and α-decay are the main decay modes in super heavy elements.

Apart from the above explained decay modes there is a signature of one more type of decay mode named proton radioactivity. The details of this type of radioactivity are explained in the next section.

1.3 Proton Radioactivity:

1.3.1 Evolution of proton radioactivity

Proton decay is the process in which nuclei decay by proton emission in complementary to its daughter nucleus. Proton emission from the nucleus was observed even before it was known that nucleus consists of protons and neutrons. At that time, they were called as H rays. A clearer picture of proton radioactivity was obtained at the beginning of 1960s by Golansky [17] and Zel'dovich [18] which was predicted by them, as an excess of proton and was expected to occur in the nuclei lying at and beyond the proton drip-line. Proton emission was observed after the β decay of ^{25}Si [17,18]. After that in 1970s, proton decay was observed from the proton unstable isomer ^{53}Co by Jackson et al. [19] and confirmed by Cerny et al [20] which led to the measurement and studies of proton radioactivity. Firstly the desired proton-rich parent nuclei are to be synthesized. These nuclei may be synthesized by methods like fragmentation, fusion evaporation reaction etc. In the first method, a stable nucleus (which is heavier than desired final product) is fragmented by a heavy ion or a proton whereas in second method, two nuclei with energies above the Coulomb barrier are brought together resulting the consequent decay of compound nucleus formed. In 1980's, ground state proton radioactivity was firstly discovered in experiments at GSI. In these experiments, Hofmann [21] identified ^{151}Lu as a spherical proton emitter with energy of about 1.23 MeV. Shortly after in an experiment at GSI second proton radioactive nucleus ^{147}Tm was observed by Klepper et al. [22]. Both ^{151}Lu and ^{147}Tm nuclei were produced by fusion-evaporation reactions, in which heavy ion beam strike on suitable target with sufficiently high energy to overcome the mutual repulsion due to their charges. ^{147}Tm isotope was produced via the fusion reaction ^{58}Ni + ^{92}Mo (E=261 MeV) producing a ^{150}Yb compound nucleus with excitation energy of E=52Mev. Then ^{150}Yb nucleus de-excite by sequential emission of neutrons, protons and gamma rays and resulting into ground state of ^{147}Tm proton emitter. In

^{151}Lu, products were separated by means of reduced velocity such as in ^{147}Tm, the decaying fragments were stopped, ionized, reaccelerated and were mass analyzed.

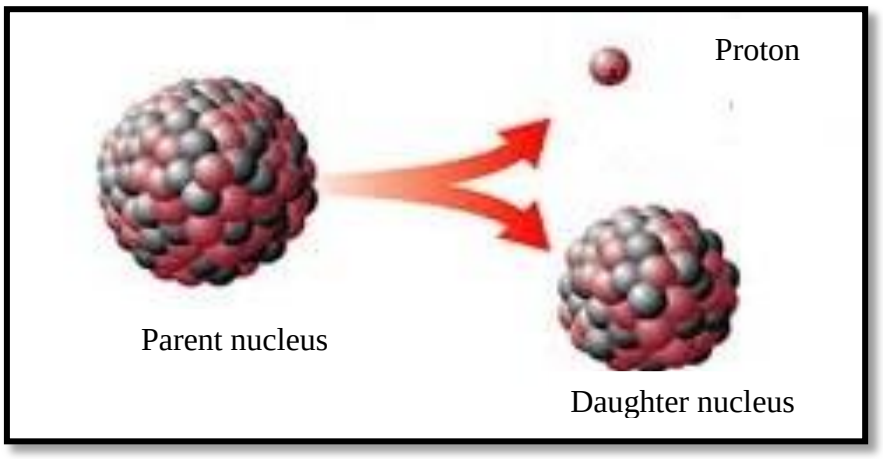

Figure 1.2: *Ground state parent nucleus spontaneously decaying into proton and daughter nucleus describing the phenomenon of proton radioactivity.*

A few years later, Faestermann et al. [23] identified proton radioactivity from ^{109}I and ^{113}Cs parent nuclei. Extensive works were performed in the 1990s at Daresbury laboratory and many new ground state proton emitters were discovered. This experimental data could be obtained due to efficient detection setups which included the use of silicon strip detectors and high-resolution separators. The studies were continued at Oak ridge national laboratory and Argonne national laboratory after the close down of the accelerator at Daresbury laboratory. In these laboratories, powerful separators combined with properly installed detection setups including double-sided silicon strip detector (DSSD) which allowed attaining high sensitivities for proton radioactivity. Till today, approximately 27 ground state spherical proton emitters have been found experimentally in which there exists 17 isomeric state proton emitters. On the other hand, if we talk about the deformed proton emitters, the number is found to be only 10 yet. For $Z \leq 50$ parent nuclei, no case of ground state proton decay has been observed, the elements which are missing between $51<Z<83$ are Te, Pm and Hg.

The proton emitters ^{109}I and ^{113}Cs were discovered at TUM (Technische Universiat Munchen) [24]. The results from them were in disagreement with spherical decay calculations. The experimental studies showed that the region of deformed nuclei existed above ^{100}Sn [25] and there were having increasing prolate deformations above Z=50 and then gradually falls while reaching Z=82. When these deformations were included in the study of ^{109}I and ^{113}Cs by Burgov and Kadmenskii during eighties and early nineties, the calculations were reasonably

in agreement with experimental results. Then at ANL in nineties, ^{131}Eu and ^{141}Ho proton emitters were discovered, again the experimental results were not reproduced by spherical calculations. Confirmation that these nuclei are deformed was done by γ spectroscopy studied. Till now approximately 10 cases of deformed nuclei have been found. Hence forth it seems that deformation effects are highly desirable to address nuclear and related dynamics.

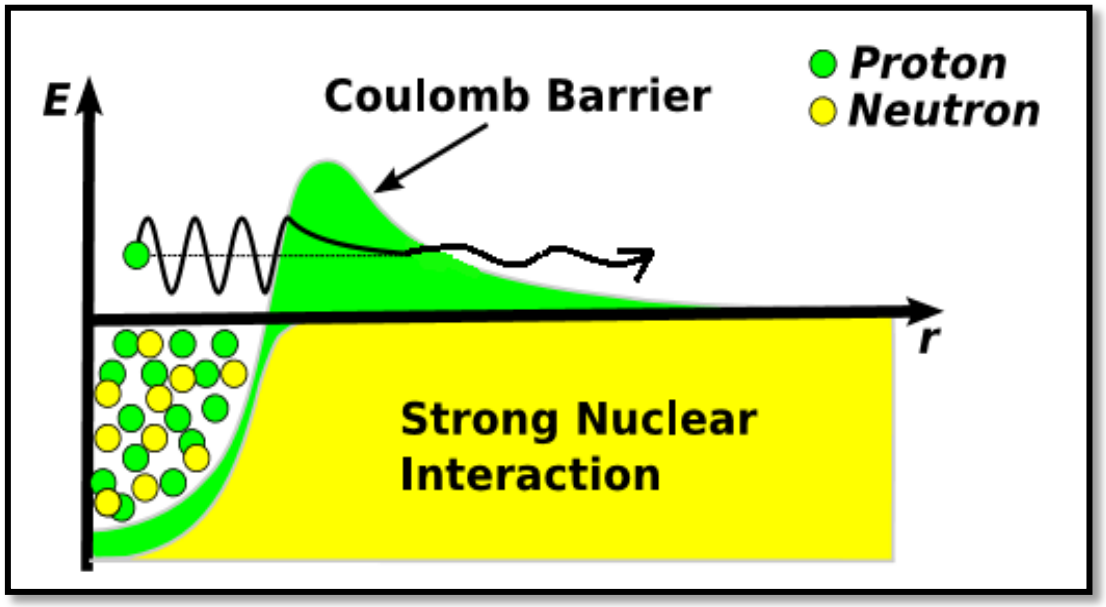

Figure 1.3: *The tunneling of proton through the Coulomb potential barrier to get emitted from the parent nucleus.*

1.3.2 Mechanism of Proton Radioactivity

In proton-rich nuclei, the potential barrier is due to superposition of Coulomb and centrifugal potential barriers (see figure 1.3). For proton decay to occur, the valence proton must tunnel quantum mechanically through the potential barrier. Classically, protons having energies less than barrier height cannot tunnel but quantum mechanically, it is possible.

Proton decay rate is sensitive to orbital angular momentum (ℓ-value) of emitted proton than α-decay. This is because of the low mass of proton than α, centrifugal potential barrier increases (which is $1/\mu$, where μ is reduced mass). So in comparison with α-decay, the centrifugal barrier seems to be important in proton decay.

Proton radioactivity gives lots of information on properties and structure of exotic nuclei. With the help of proton radioactivity, unknown regions of the periodic table can be explored and through studies of exotic nuclei many fundamental properties of nuclear physics can be explored. The mass of some unbound nuclei in atomic mass evaluation tables (also used in present work for binding energies) have been determined by proton decay measurements. Apart from proton radioactivity, radioactive beams are also found to be helpful in forming the proton rich nuclei which lie beyond the proton drip-line. The motivation for the construction of more advanced radioactive beams is to explore new regions on the proton and neutron-rich side and to have complete knowledge of nuclear drip-lines. On the other hand, the inverse reaction of proton radioactivity i.e. proton capture plays an important role in nuclear astrophysics, so the study of proton radioactivity dynamics is of huge importance and relevance.

1.4 Deformations and orientations:

It is noticeable from the literature that the deformation effects play an important role in the decay process of nuclear systems. So, it is essential to investigate the role of the deformed structure in nuclear decay if the system possesses some degree of deformation. Not only the shape of parent nucleus is crucial in decay mechanism, but the participation of the shape degree of freedom of daughter and cluster is also of equal important.

Deformations in nuclei were considered to account for discrepancies in quadrupole moment (i.e. measured quadrupole moment was larger than predicted one). So, to resolve the discrepancies relevant models were developed. According to collective nuclear model, in odd-A nuclei, the loosely bound nucleon polarizes the even-even core which lead to spheroid shape rather than spherical shape. Individual nucleons are imagined to move in orbits and the potential distribution inside nucleus is determined by remaining nucleons. The entire shell configuration undergoes oscillations in shape. Potential of the region in which particles move, get modified due to shell oscillations accompanied in the deformed nuclei. If the nuclei consist of almost closed shells (or at magic number), the core is stable and hence, the oscillations are small and the nuclei are generally spherical/near spherical. There are nucleonic, vibrational and rotational states of nucleus. Rotations and vibrations arise from the motion of nuclear core and nucleonic states arise due to motion of loosely bound nucleons. The collective motion of deformed nucleus can be seen as vibration or oscillation about equilibrium shape, and rotation of nuclear mass.

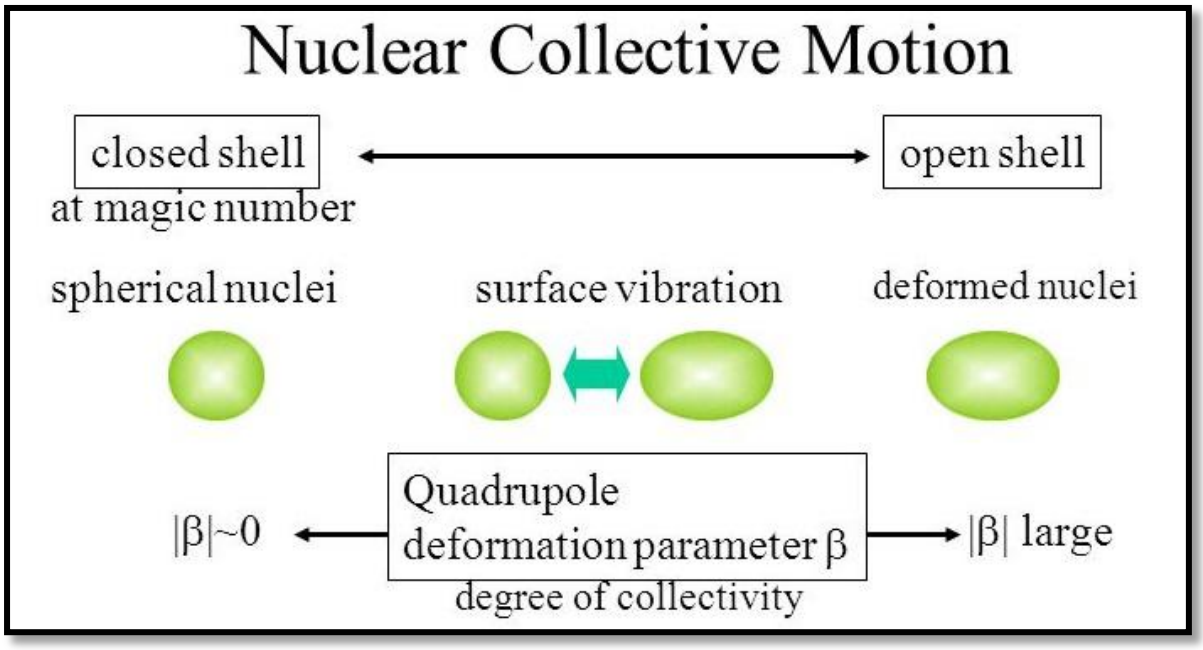

Figure 1.4: *Nucleus get deformed due to the presence of surface vibrations according to nuclear collective model.*

According to unified fission model (deformed shell model), the vibrational and rotational motion is due to motion of entire nucleus and the nucleus as a whole looks like a liquid drop. According to this model, nucleus is not a rigid body, the loosely bound nucleons set up tensions in the core and the nucleus under consideration gets polarized. If the force between loosely bound nucleons and core is attractive, oblate shape of nucleus is formed and if repulsive, then prolate shape is formed. The deformations which lead to oblate and prolate shapes are known as quadrupole deformations.

The shape of the nucleus can be investigated by determination of quadrupole moment (β_2) of the nucleus. Quadrupole moment can be calculated by analysis of the hyperfine structure of atomic spectra or by electron scattering experiments. The quadrupole moment gives the deviation of nuclear charge distribution from spherical shape and can be written a

$$Q = \frac{2}{5} Z \int (a^2 - b^2)$$

Q is equal to 0 (zero) for spherically symmetric charge distribution. If Q is positive, the shape of nuclei becomes prolate and if Q is negative, the shape of nuclei is oblate as depicted in figure 1.5.

Degree	Deformations	Nuclear Shapes
λ=1	Spherical	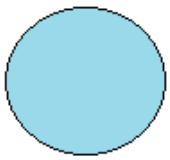
λ=2	Quadrupoles β_2	-ve β_2  Oblate +ve β_2 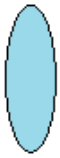 Prolate
λ=3	Octupoles β_3	
λ=4	Hexadecapoles β_4	 +ve β_4 Belly-out -ve β_4  Belly-in

Figure 1.5: *Degree of deformations shown along with their corresponding shapes.*

The degree to which the nucleus is deformed can be given by deformation para-meter represented by β_λ where λ represent the degree of deformation. The value of λ can be 2, 3, 4 depending upon the extent of deformation i.e. λ=2 for quadrupole, λ=3 for octupole, λ=4 for hexadecapole. The higher order deformations like octupole (pear shaped) and hexadecapole are also represented in figure 1.5. The contribution of these higher multipole deformations along with the choice of appropriate orientations leads to enormous exotic nuclear shapes. But the present work is limited to quadrupole deformations only.

Orientations relate the shape of nuclei to the angles between symmetry and collision axis. It basically tells how the nuclei are oriented when they are on the verge of separation during decay. For quadrupole deformations, it can be compact or elongated (for details see figure[1.3] of ref [26]) The 'hot compact' configuration is the one in which the interaction radius is small and barrier high, whereas the 'cold elongated' configuration corresponds to largest interaction radius and lowest interaction barrier. In proton decay, proton and daughter nuclei are emitted, so at the verge of separation, proton is surely spherical and daughter may or may not be deformed.

Deformations and orientations are extremely useful to understand the nuclear structure and dynamics at extreme conditions thereby providing important information for future experiments. The inclusion of deformations and orientations affects the decay rates, for example in fusion reactions, due to deformed shape of nuclei, its barrier height gets lowered which provides an easier path for compound nucleus formation. Similarly, orientations change the Coulomb barrier as well as the distance between centers of colliding nuclei. So, whenever deformed configuration is considered orientation degree of freedom becomes extremely desirable.

1.5 Spherical and deformed proton emitters

A parent nucleus which emits proton spontaneously can be spherical as well as deformed. As the proton radioactivity deals with exotic nuclei which are unstable, so deformations can no longer be ignored. Mostly, the decay rate of proton emission is estimated by considering nuclei as spherical but calculations are done by treating them as deformed for nuclei in transitional region beyond Z=50 shell closure (^{109}I and ^{112,113}Cs) and in region of light rare earth nuclei (^{131}Eu and ^{140,141}Ho). Heavy nuclei emit protons to lower their energy and rearranging their protons and neutrons into deformed shells accommodating different number of nucleons.

The same theoretical approach can be used for spherical and deformed proton emitters but using the deformation parameters in the theoretical approach for latter. Presently, preformed cluster model (PCM) has been used to deal with ground states of spherical and deformed proton emitters. Proton radioactivity is generally a phenomenon for odd Z nucleus and for even Z nuclei, two proton radioactivity is most common [27]. In the present work, the experimental as well as theoretical data for spherical proton emitters, is taken from ref. [28-29] and for deformed proton emitters the data is taken from ref [28, 30, 31]. Tables for spherical and deformed proton emitters are shown below:

Table1.1: *Experimental logarithm of half lives, Q_P values and ℓ values of proton decay from different spherical proton emitters [28]*

S.No.	Parent nucleus	ℓ ($\hbar$)	Q_P(Mev)	$Log_{10}T_{1/2}$(Exp.) (sec)
1	^{105}Sb	2	0.491	2.049
2	^{145}Tm	5	1.753	-5.409
3	^{147}Tm	5	1.071	0.591
4	^{150}Lu	5	1.283	-1.180
5	^{151}Lu	5	1.255	0.896
6	^{155}Ta	5	1.791	-4.921
7	^{156}Ta	2	1.028	-0.620
8	^{157}Ta	0	0.947	-0.523
9	^{160}Re	2	1.284	-3.046
10	^{161}Re	0	1.214	-3.432
11	^{164}Ir	5	1.844	-3.959
12	^{166}Ir	2	1.168	-0.824
13	^{167}Ir	0	1.086	-0.959
14	^{171}Au	0	1.469	-4.770
15	^{177}Tl	0	1.18	-1.174
16	^{185}Bi	0	1.624	-4.229

1.6 Role of Binding Energies:

Binding energy is the energy equivalent to the mass defect. It is basically the energy needed to hold or bind the nucleons together inside the nucleus. Radioactive decay occur if the product nucleus has nuclear binding energy greater than the initial decaying nucleus or it occurs in unstable nucleus that doesn't have enough binding energy to hold the nucleons together due to an excess of either protons or neutrons. Binding energies play very important role in decay characteristics i.e. decay half lives, Q-value and decay rates. In the study of Proton Radioactivity with PCM, binding energies change the total fragmentation potential which leads to the change of parameters in schrödinger equation and its solution (preformation probability) and hence the decay constant and half life for the nuclear system gets accordingly modified. Hence in proton radioactivity, correct selection of binding energies is very essential. In present work, old data on binding energies [32] is replaced by

new experimental data on binding energies [33], in other words present work is carried out by using latest available binding energies [33].

Table1.2: *Experimental logarithm of half lives, Q_P values and ℓ values of proton decay from different deformed proton emitters [28, 30, 31].*

S.No.	Parent nucleus	$\ell(\hbar)$	Q_P(Mev)	$Log_{10}T_{1/2}$(Exp) (sec)
1	^{109}I	2	0.830	-3.987
2	^{112}Cs	2	0.830	-3.301
3	^{113}Cs	2	0.980	-4.777
4	^{117}La	2	0.811	-1.602
5	^{121}Pr	2	0.851	-2.000
6	^{130}Eu	2	1.033	-3.046
7	^{131}Eu	2	0.953	-1.575
8	^{135}Tb	3	1.193	-3.027
9	^{140}Ho	3	1.110	-2.222
10	^{141}Ho	3	1.194	-2.387

Nuclear properties are of two types, one is related to nuclei at rest and another is related to its motion or dynamics. Reaction mechanism exhibiting differential cross-sections are employed to address dynamical behavior of nuclear systems. The ground state masses, deformations, decay half lives, decay modes, all come under the static properties of nucleus, with which we will be dealing in present work. The first atomic mass evaluation was published in 1993 [34] by G. Audi and A.H. Wapstra and then second in 1995 [35] and then in 2003 [32]. After the evolution of experimental atomic mass evaluation 2003, large amount of high quality, accurate data has been published as atomic mass evaluation in 2012 which is used in present work. The experimental techniques which were used to extract the data are direct spectrometry measurements using penny traps and γ-ray energy measurement following neutron capture reaction. Penny trap method is very accurate and data extracted from it is useful because it gives masses of unstable short lived nuclei. In atomic mass evaluation 2012, data from both the experimental techniques is combined which improves the precision of

atomic masses. In AME, the best masses of all the experimental data from all sources are chosen by some mathematical tools (firstly the data is used in mass difference equations and then least square fitting is done) and computer tools (for graphical display). The unknown masses are determined by trends in mass surface (TMS) in neighborhood. When atomic masses are plotted against N and Z, a three dimensional surface is obtained called as mass surface. So, the unknown masses can be made known by extrapolating the well known masses on same surface.

1.7 References:

1. images .slideshare.com/26/8389466/slides/slide_10.jpg
2. Pierre de Marcillac, Noe¨l Coron, Ge´rard Dambier, Jacques Leblanc & Jean-Pierre Moalic, Nature 422, 876 (2003).
3. A. Sandulescu, D.N. Poenaru, W. Greiner, Sov. J. Part. Nucl. II, 528 (1980).
4. H.J. Rose, G.A. Jones, Nature 307, 245 (1984).
5. G.Sawhney and M. K. Sharma, Raj K. Gupta Phys. Rev C 83, 064610 (2011).
6. D. N. Poenaru and W. Greiner, J. Phys. G: Nucl. Part. Phys. 17, 443 (1991).
7. R.K. Gupta, M. Balasubramaniam, R. Kumar, D. Singh, C. Beck, and W. Greiner, Phys. Rev. C 71, 014601 (2005).
8. B. B. Singh, M. K. Sharma, R. K. Gupta, and W. Greiner, Int. J. Mod. Phys. E15, 699 (2006).
9. R.K. Gupta, M. Balasubramaniam, R. Kumar, D. Singh, S. K. Arun and W. Greiner, J. Phys. G: Nucl. Part. Phys. 32, 345 (2006).
10. D.N. Poenaru and W.Greiner Phys. Rev. C 47, 5 (1993).
11. S. Kumar, Dharam Bir and Raj K.Gupta Phy. Rev. C 51, 4 (1995).
12. S.Kumar, J.S Batra and R.K Gupta J. Phys. G: Nucl. Part. Phys. 22, 215 (1996).
13. D.N poenaru, R.A. Gherghescu, W. Greiner, Phys. Rev. Lett 107, 062503 (2011).
14. N.Bohr and J.A.Wheeler, Phys. Rev 56, 426 (1939).
15. G.N flerov and K.A. petrzhak Phys. Rev. 58, 89 (1940).
16. N.E Holden and D.C Hoffman Pure Appl. Chem, 72, 8 PP.1525 (2000).
17. V.I. Goldansky, Nucl. Phys. 19, 482 (1960).
18. Y.B Zel'dovich, Sov. Phys. JETP II, 812, 154 (1960).
19. K.P.Jackson, C.U.Cardinal, H.C.Evans, N.A.Jelley and J.Cerny, Phys. Lett. B206, 592 (1993).
20. J.Cerny, J.E Esterl, R.A.Gough, R.G.Sextro, Phys.Lett.B33, 284 (1970).
21. S. Hofmann, W. Reisdorf, G. M¨unzenberg, F. Hessberger, J. Schneider, P. Armbruster, Z. Phys. A305, 111, 154, 156, 159 (1982).
22. O.Klepper, T.Batsch, S.Hofmann, R.Kirchner, W.Kurcewicz, W.Reisdorf, E.Roeckl, D.Schardt and G.Nymen, Z. Phys A 305, 125 (1982).
23. T.Faesterman, A.Gillitzer, T.Hartel, P.Kienle and E.Nolte, Phys.Lett. B137,23 (1984).
24. A.Gillitzer et al. Z. Phys. A 326, 107 (1987).
25. R.K.Shelina, T.Sikkeland and R.N. Chanda, Phys. Rev. Lett. 7, 446 (1961).

26. http://dspace.thapar.edu:8080/jspui/handle/10266/3570
27. http://www.euroschoolonexoticbeams.be/site/files/nlp/LNP764_contrib5.pdf
28. A. A. Sonzogni, Nuclear Data Sheets 95, 1 (2002).
29. M. Balasubramaniam and N. Arunachalam, Phys. Rev. C 71, 014603 (2005).
30. P. J. Woods et al., Phys. Rev. C 69, 051302(R) (2004).
31. A. P. Robinson et al., Phys. Rev. Lett. 95, 032502 (2005).
32. A. H. Wapstra, G. Audi and C.Thibault, Nucl. Phys.A 729 129 (2003).
33. M. Wang, G. Audi, A.H. Wapstra, F.G. Kondev, M. MacCormick, X. Xu1, and B. Pfeiffer, Chin. Phys. C, 36, 12 (2012).
34. G.Audi and A.H. Wapstra, Nucl. Phys.A 565 (1993).
35. G.Audi and A.H. Wapstra, Nucl. Phys.A 595 (1995).

Chapter 2

Methodology

Chapter 2

2.1 Introduction

Various theoretical attempts have been made to study the proton radioactivity and nuclear structure beyond the border of nuclear stability. The examples of such theoretical attempts for spherical proton emitters are PCM as unified fission model [1], distorted wave born approximation [2], two potential approach [2], simple description of barrier penetration problem in terms of one dimensional quasi classical methods [2] and in some cases the results are obtained by changing the potentials [3]. The basic idea behind born approximation, two potential approach and quasiclassical methods is that the proton emitters are considered as extremely narrow resonances. But, The decay width for the resonances which yield the proton partial half life, are taken different in different methods. For deformed proton emitters coupled channel approach is used. In this approach, the decaying system i.e unbound proton interacting with deformed core can be interpreted as a particle rotor system.

In our work, theoretical approach preformed cluster model [PCM] has been used for spherical as well as deformed proton emitters. According to this theoretical premise, the daughter and cluster (proton in this case) is supposed to be preborn in parent nucleus. It then strikes the walls of nucleus with frequency known as assault frequency and finally penetrates through the potential barrier and gets emitted. There are two probabilities with which we will be dealing one is preformation probability (probability of daughter or cluster to be preformed) and another is penetration probability (probability of cluster to get penetrated through potential barrier). These probabilities help in half life calculations. The preformed cluster model is based on Quantum Mechanical Fragmentation Theory (QMFT) as explained below:

2.2 Quantum Mechanical Fragmentation Theory (QMFT)

The *QMFT* [4-9] is used to describe the processes which involve fusion as well as fission. In *QMFT* concept of probability is utilized to explore the possible effect of shell closure on different decay mechanisms. The *QMFT* is worked out in terms of R, $\beta_{\lambda i}$, θ_i, φ, ε and η parameters. Where R is separation between two fragments, $\beta_{\lambda i}$ are the deformation coordinates, θ_i is the angle of orientation, φ is the azimuthal angle, ε is the neck parameter

and η is the asymmetry in the emitted fragments which may be charge asymmetry η_Z or mass asymmetry η_A [10-12] shown by expressions given below:

$$\eta_A = \frac{A_1 - A_2}{A_1 + A_2} \quad \text{and} \quad \eta_Z = \frac{Z_1 - Z_2}{Z_1 + Z_2} \tag{2.1}$$

Here $A = A_1 + A_2$ and $Z = Z_1 + Z_2$. A, N and Z are respectively the mass, neutron and charge number of the composite system.

Schrodinger wave equation for co-ordinates η can be written as follows,

$$\left\{ -\frac{\hbar^2}{2\sqrt{B_{\eta\eta}}} \frac{\partial}{\partial \eta} \frac{1}{\sqrt{B_{\eta\eta}}} \frac{\partial}{\partial \eta} + V_R(\eta) \right\} \psi^v(\eta) = E_R^v \psi^v(\eta) \tag{2.2}$$

With

$$\psi(\eta, R) = \psi(\eta)\ \psi(R) \tag{2.3}$$

And

$$E = E_\eta + E_R \tag{2.4}$$

We have taken η dependence of E and ψ. The states $\psi^v(\eta)$ are the vibrational states in the potential $V(\eta)$ where v = 0, 1, 2, ... In our case, for ground state decays, it is zero. The Schrodinger equation eqn. (2.2) is used to calculate the preformation probability (P_0) of the fragments inside the nucleus before the occurrence of decay. Once the clusters/fragments are preformed, WKB approximation can be used to calculate the probability of penetration (P) of fragments/clusters across the barrier. On the basis of this concept, PCM was proposed in [13-17], which was formulated to understand the decay processes in which fragments get emitted from the ground state of parent nucleus. The deformation and orientation effects are duly incorporated in the formalism.

2.2.1 The Fragmentation potential V (η)

The potential required to solve the Eq. (2.2) is given by equation (2.5) known as

fragmentation potential. The expression of fragmentation potential used in PCM which includes deformations and orientations is given by:

$$V_R(\eta) = -\sum_{i=1}^{2}[B_i(A_i, Z_i)] + V_c(R, Z_i, \beta_{\lambda i}, \theta_i) + V_p(R, A_i, \beta_{\lambda i}, \theta_i) + V_l(R, A_i, \beta_{\lambda i}, \theta_i) \quad (2.5)$$

Where B_i are the binding energies of fragments. V_C is the Coulomb potential, V_P is the nuclear proximity potential and V_ℓ is the potential due to angular momentum. All the three potentials are explained in later sections.

The fragmentation potential $V(\eta)$ in PCM is calculated in terms of R which is fixed at the touching configuration i.e. at $R=C_t=C_1+C_2$, the C_i being the Sussmann central radii $C_i=R_i - 1/R_i$ (in fm) with R_i as the equivalent spherical radii R_{0i} (eqn. 2.7).

$$R_i(\alpha_i) = R_0[1 + \sum_\lambda \beta_{\lambda i} Y_\lambda^{(0)}(\alpha_i] \quad (2.6)$$

And

$$R_{0i} = [1.28A_i^{1/3} - 0.76 + 0.8A_i^{-1/3}] \quad (2.7)$$

Here λ = 2,3,4..., and α_i represents the angle between the radius vector R_i of the colliding nuclei and symmetry axis (see Fig. 2.2 from ref. [18]), measured clockwise.

2.2.2 The Coulomb potential

When two charged particles interact with each other, a potential called coulomb potential comes into the picture. The Coulomb potential for the interaction between two spherical nuclei is given as:

$$V_C = \frac{Z_1 Z_2 e^2}{R} \quad (2.8)$$

Different authors [19,20] gave different expressions for Coulomb potential to introduce the effect of deformations and orientations. The expression used in PCM from ref. [19] is given as:

$$V_C(R, Z_i, \beta_{\lambda i}, \theta_i,) = \frac{Z_1 Z_2 e^2}{R} + 3Z_1 Z_2 e^2 \sum_{\lambda, I=1,2} \frac{R_i^{\lambda}(\alpha_i)}{(2\lambda+1)R(T)^{\lambda+1}} Y_{\lambda}^{(0)}(\theta_i) \left[\beta_{\lambda i} + \frac{4}{7}\beta_{\lambda i}^2 Y_{\lambda}^{(0)}(\theta_i)\right] \quad (2.9)$$

Where R_i is given by Eq. (2.6) and $Y_{\lambda}^{(0)}(\theta_i)$ represents the spherical harmonic function.

2.2.3 The Proximity Potential-77

When the parent nucleus is on the verge of decay into two fragments, the distance between two nuclei is approximately equal to the surface thickness of interacting nuclei. At that time surfaces of both the decaying fragments are in contact with each other due to which an attractive force arises between the two surfaces known as proximity force. The potential associated with this force is known as proximity potential. Blocki et al. [21] by reanalyzing and extending a theorem, which was originally given by Deryagin [22] gave a statement, according to which, when two gently curved surfaces are in close proximity then the force between them is proportional to the interaction potential per unit area between the two flat surfaces. Expression of Prox-77 for deformed and oriented nuclei [23] is given as:

$$V_P(R, A_i, \beta_{\lambda i}, \theta_i) = 4\pi R \gamma b \phi(s_0) \quad (2.10)$$

where γ and b are given by

$$\gamma = 0.9517 \left[1 - 1.7826 \left(\frac{N-Z}{A}\right)^2\right] MeV\ fm^{-2} \quad (2.11)$$

$$b = \left[\pi/2\sqrt{3} ln 9\right]_{t_{10-90}} \quad (2.12)$$

And for $s_0 \leq 1.2511$ and $s_0 \geq 1.2511$, $\Phi(s_0)$ is given by:.

$$\phi(s_0) = \begin{cases} -\frac{1}{2}(s_0 - 2.54)^2 - 0.0852(s_0 - 2.54)^3 \\ -3.437\exp\left(-\frac{s_0}{0.75}\right) \end{cases} \quad (2.13)$$

γ is the nuclear surface tension, b (approx. 1fm) is the diffuseness of nuclear surface, t_{10-90} is the surface thickness upto which the density profile changes from 90% to 10% and $\Phi(s_0)$ used in Eq. (2.10) is the universal function which depends on the distance of closest approach s_0. This function is defined for -ve (the overlap region), zero (touching configuration) and +ve values of s_0.

2.2.4 Potential due to angular momentum

The nucleons inside the nucleus exhibits rotational motion, which give rise to the angular momentum ℓ. The potential which arises due to this rotational motion is given:

$$V_\ell(R, A_i, \beta_{\lambda i}, \theta_i) = \frac{\hbar^2 \ell(\ell+1)}{2I(T)} \quad (2.14)$$

This potential is inversely proportional to the moment of inertia I , defined as:

$$I_s(T) = \mu R^2 + \frac{2}{5} A_1 m R_1^2(\alpha_1, T) + \frac{2}{5} A_2 m R_2^2(\alpha_2, T) \quad (2.15)$$

in which reduced mass $\left(\mu = \frac{A_1 A_2}{A_1 + A_2} m\right)$ is also involved in addition to individual masses.

2.2.5 Scattering Potential V (R)

The scattering potential $V(R)$ is defined as the sum of proximity, coulomb and centrifugal potentials. The expression of potential involving the effect of deformations and orientations is given as:

$$V_R(A_i, R, \ell) = V_P(R, A_i, \beta_{\lambda i}, \theta_i) + V_C(R, Z_i, \beta_{\lambda i}, \theta_i) + V_\ell(R, A_i, \beta_{\lambda i}, \theta_i) \quad (2.16)$$

2.3 The Preformed Cluster Model

PCM was formulated to understand the process of cluster/fragments emission from the ground state of parent nuclei. Also, the ground state decay phenomena have been studied with other theoretical approaches like Unified fission model (UFM) etc. The presumptions of UFM

and PCM (used in present work) formalisms are completely different. In UFM [24, 25], which is the fission model, the fragments/clusters preformation is given by the penetrability of the internal part of the barrier. On the other hand, in PCM the Schrodinger wave Eq. (2.4) is solved to obtain preformation probability P_0 which is different for different clusters. In PCM, there is no restriction on the calculations of P_0 but in Models like Blendowske et al. [26, 27], P_0 can be calculated for the mass of cluster/fragment up to A = 28 only. PCM [13-17] has been developed by adopting mainly the Gamow's theory [28] of α-decay. In PCM more realistic nuclear potential i.e the nuclear proximity potential is used rather than simple square well potential.

The decay constant, hence decay half-life are given as:

$$\lambda^{PCM} = P\, \upsilon_0\, P_0, \qquad T_{1/2} = ln2/\lambda \tag{2.17}$$

Here P is penetrability and υ_0 is assault frequency given by:

$$\upsilon_0 = \upsilon/R = \frac{\left(2E_2/\mu\right)^{1/2}}{R} \tag{2.18}$$

where R is the radius of parent nucleus and E_2 is the kinetic energy of the emitted fragment/cluster.

2.3.1 Preformation probability P_0

The Schrodinger wave Eq. (2.2) in η-coordinate, can be solved to obtain P_0 which is used in eqn. (2.17). So probability P_0 of finding the mass fragment η at fixed R on decay path is proportional to:

$$P_0(A_2) \propto |\psi^{\nu}(A_2)|^2 \qquad \nu = 0,1,2\ldots. \tag{2.19}$$

For ground state decays such as proton decay, α decay, spontaneous fission or cluster decay, only the lowest vibrational state $\nu = 0$ is occupied.

2.3.2 Penetration probability *P*

The penetrability P is obtained by solving the WKB integral between R_a (the first turning point) and R_b (second turning points) (Fig. 2.1). The tunneling begins at $R = R_a$ and

terminates at $R=R_b$, with $V(R_b) = Q$-value for ground state decay. Thus, as per fig. 2.1, the transmission probability P consists of the following three contributions:

1. The penetrability P_i from R_a *to* R_i,
2. The (inner) de-excitation probability W_i at R_i, and
3. The penetrability P_b from R_i to R_b giving the penetration probability as:

$$P = P_i W_i P_b \tag{2.20}$$

Following the excitation model of M.Greiner and W. Scheid, we take the de-excitation probability W_i=1 for a heavy cluster decays, which reduces Eq.(2.20) to the following:

$$P = P_i P_b \tag{2.21}$$

where P_i and P_b in WKB approximation are

$$P_i = \exp\left[-\frac{2}{\hbar}\int_{R_a}^{R_{ii}}\{2\mu[V(R)-V(R_i)]\}^{1/2}dR\right] \tag{2.22}$$

$$P_b = \exp\left[-\frac{2}{\hbar}\int_{R_i}^{R_b}\{2\mu[V(R)-Q]\}^{1/2}dR\right] \tag{2.23}$$

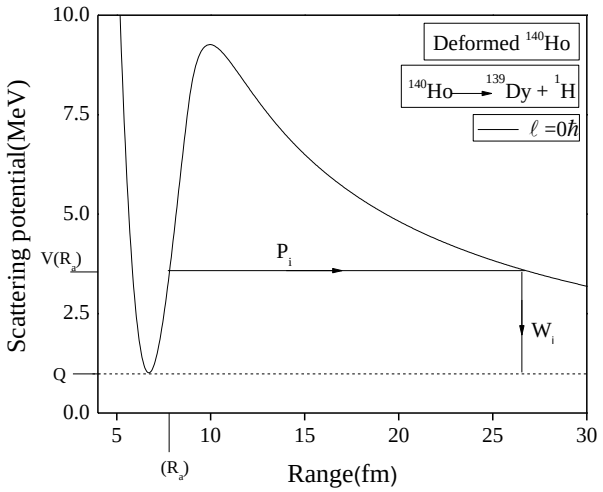

Figure 2.1: The *scattering plot for proton decay of ^{140}Ho into ^{139}Dy at $\ell = 3$.*

For R_a, we use the below given expression

$$R_a(\eta) = C_1(\alpha_1) + C_2(\alpha_2) + \Delta R$$

$$= C_t(\alpha, \eta) + \Delta R \tag{2.24}$$

Where ΔR is a parameter incorporating the neck formation effects.

By using the methodology above, we intend to address proton radioactivity dynamics by adopting spherical as well as deformed fragmentation approaches. The results are discussed in subsequent chapter.

2.4 References:

1) M. Balasubramaniam and N. Arun Phys. Rev. C 71, 014603 (2005).
2) S. Aberg, P. B. semmes and W. Nazarewicz Phys. Rev. C 56, 1762 (1997).
3) I. Mehrotra, S. Prakash Indian Journal of Pure and applied physics 46, PP 312-314 (2008).
4) R. K. Gupta, R. Kumar, N. K. Dhiman, M. Balasubraniam, W. Scheid, and C. Beck, Phys. Rev. C 68, 014610 (2003).
5) M. Balasubraniam, R. Kumar, R. K. Gupta, C. Beck, and W. Scheid, J. Phys. G 29, 2703 (2003).
6) R. K. Gupta, M. Balasubraniam, R. Kumar, D. Singh, and C. Beck, Nucl. Phys. A 738, 479 (2004).
7) R. K. Gupta, M. Balasubramaniam, R. Kumar, D. Singh, C. Beck, and W. Greiner, Phys. Rev. C 71, 014601 (2005).
8) B. B. Singh, M. K. Sharma, R. K. Gupta, and W. Greiner, Int. J. Mod. Phys. E15, 699 (2006).
9) R. K. Gupta, M. Balasubramaniam, R. Kumar, D. Singh, S. K. Arun and W. Greiner, J. Phys. G: Nucl. Part. Phys. 32, 345 (2006).
10) J. Maruhn and W. Greiner, Phys. Rev. Lett. 32, 548 (1974).
11) H. J. Fink, W. Greiner, R. K. Gupta, S. Liran, J. H. Maruhn, W. Scheid, and O. Zohni, in Proceedings of Int. Conf. on Reaction between Complex Nuclei, Nashville, 1974, 21, (Amsterdam: North Holland), page 2.
12) R. K. Gupta, W. Scheid, and W. Greiner, Phys. Rev. Lett. 35, 353 (1975).
13) S. S. Malik, R. K. Gupta, Phys. Rev. C 39, 1992 (1989).
14) S. Kumar and R. K. Gupta, Phys. Rev. C 55, 218 (1997).
15) S. K. Arun, R. K. Gupta, S. Kanwar, B. B. Singh, and M. K. Sharma, Phys. Rev. C 80, 034317 (2009).
16) G. Sawhney, M. K. Sharma, and R. K. Gupta, Phys. Rev. C 83, 064610 (2011).
17) R. Kumar and M. K. Sharma, Phys. Rev. C 85, 054612 (2012).
18) http://dspace.thapar.edu:8080/jspui/handle/10266/3570
19) R. K. Gupta, M. Balasubramaniam, R. Kumar, N. Singh, M. Manhas, and W. Greiner, J. Phys. G: Nucl. Part. Phys. 31, 631 (2005).
20) M. Munchow, D. Hahn, and W. Scheid, Nucl. Phys. A 388, 381 (1982).
21) J. Blocki, J. Randrup, W. J. Swiatecki, and C. F. Tsang, Ann. Phys. 105, 427 (1977).

22) Deryagin, Z.Kolloid 69, 155 (1934).
23) R. K. Gupta, N. Singh, and M. Manhas, Phys. Rev. C 70, 034608 (2004).
24) G. A. Pik-Pichak, Fiz. Elem. Chastits At. Yadra 44, 1421 (1986).
25) D. N. Poenaru, M. Ivascu, A. Sandulescu, and W. Greiner, Phys. Rev. C 32, 572 (1985).
26) R. Blendowske, T. Fliessbach, and H. Walliser, Nucl. Phys. A 464, 75 (1987).
27) R. Blendowske and H. Walliser, Phys. Rev. Lett. 61, 1930 (1988).
28) G. Gamov, Z. Phys. 51, 204 (1928).

Chapter 3

Results & Conclusions

Chapter-3

Results and Discussions

3.1 Introduction:

In the present work, we planned to assess the impact of new binding energies [1] on proton decay characteristics i.e. half life, penetrability, preformation probability etc via proper inclusion of deformation effects of the fragmentation process. The results presented in this thesis are for 14 cases of spherical proton emitters whose atomic mass lies in the range 145 to 185 and 10 cases of deformed proton emitters whose mass lies in between 109 and 141. The binding energies are taken from Audi et al. [1] and the values of deformations are employed in reference to Moller et al. [2]. The variation of fragmentation potential and preformation factor is analyzed as a function of fragment mass, at different ℓ-values for spherical as well as deformed proton emitters. We shall see that when deformations are included, the potential energy surfaces get greatly affected emphasizing the fact that deformations play significant role in the considered nuclear dynamics. The shell effects in deformed as well as spherical proton emitters are also seen. The barrier characteristics behavior of proton decay is compared with alpha decay for ^{185}Bi parent nucleus. The standard deviation (between experimental and calculated half lives) is calculated for both spherical as well deformed proton emitters. It may be noted here that, the preformed cluster decay model (PCM) is used to reproduce the available experimental data on half lives of spherical as well as deformed proton emitters.

The input data used for calculations comprises of available experimental information on ℓ values, new binding energies [1], and deformations for deformed systems. All the spherical proton emitters shown in table 3.1, represent the preformation probabilities (P_0), penetrability (P), Q value, neck length parameter ΔR, experimental half lives ($\log_{10}T_{1/2}$) and PCM calculated half lives.

3.2 Results and discussion

Table 3.1: *Spherical proton emitters measured so far with experimental ℓ and Q values and calculated values of P_0, P, half lives (calculated with old and new binding energies).*

Sr. No	Parent nuclei	ℓ (ħ)	ΔR (fm)	Preformation Probability ($\log_{10} P_0$)	Penetrability ($\log_{10} P$)	$\log_{10} T_{1/2}$(s)			Q_P (MeV)
						Expt.	PCM		
							B.E[4]	B.E[1]	
1	^{145}Tm	5	-0.6	-5.069	-10.810	-5.409	-5.170	-5.755	1.742
2	^{147}Tm	5	-0.5	-5.253	-16.332	0.591	1.095	0.190	1.060
3	^{150}Lu	5	-0.9	-4.435	-14.709	-1.180	-0.859	-2.340	1.272
4	^{151}Lu	5	-1.0	-4.728	-14.854	-0.896	-0.573	-1.973	1.242
5	^{155}Ta	5	-0.2	-4.119	-13.459	-4.921	-4.637	-4.007	1.452
6	^{156}Ta	2	0.33	-3.194	-17.657	-0.620	-0.461	-0.656	1.022
7	^{157}Ta	0	0.39	-2.671	-18.150	-0.523	-0.126	-0.668	0.942
8	^{160}Re	2	0.55	-3.130	-15.369	-3.046	-3.109	-3.052	1.272
9	^{161}Re	0	0.33	-3.809	-13.816	-3.432	-3.231	-3.723	1.202
10	^{164}Ir	5	0.48	-3.564	-17.206	-3.959	-4.193	-3.967	1.562
11	^{166}Ir	2	0.56	-2.328	-18.245	-0.824	-1.160	-0.813	1.162
12	^{167}Ir	0	0.28	-2.714	-14.027	-0.959	-0.943	-0.894	1.071
13	^{177}Tl	0	0.2	-2.873	-17.607	-1.174	-0.993	-1.035	1.160
14	^{185}Bi	0	0.2	-2.914	-14.524	-4.229	-5.184	-4.130	1.524

Above table represents the different spherical proton emitters which are observed experimentally [3]. The details such as ℓ value, Q-value, experimental and PCM calculated half lives are also shown with their corresponding preformation probabilities, tunneling probabilities and neck lengths behavior. To address proton decay with collective clusterization process in PCM, we have studied total 14 cases of spherical proton emitters, having angular momentum range ℓ=0 to 5. Computed half lives are analogize nicely with experimental data. It has been found that present calculations using new binding energies [1] shoe relatively better comparison with data those using old binding energies [4]. The standard rms deviation from the experimental data for the above spherical proton emitters is also calculated using formula [5]:

$$\sigma = \sqrt{\left[\frac{\sum_{i=1}^{n}[\log_{10}(T_i/T_{Exp})]^2}{n-1}\right]}$$

The value for the standard rms deviation is found to be 1.231, which simply means that the present systematic gives satisfactory description of the proton decay. Figure 3.1 shows the change of fragmentation potential with fragment mass for different spherical proton emitters plotted using spherical approach. The three panels in the graph show the variation of fragmentation potential for different parent nuclei at three different ℓ values i.e. ℓ=0ħ, 2ħ, 5ħ as shown in table 3.1. First of all, it can be seen from graph that on increasing the mass of parent nucleus, the magnitude of fragmentation potential increases. Higher the mass of parent nucleus, higher is the fragmentation potential. Also, in every case, there is a competition of proton decay with alpha decay as seen from the potential deep minima's that are marked in figure. It means that there is equally good probability of alpha radioactivity in the above cases. A comparative study of proton radioactivity vs. alpha radioactivity is also carried out for one of the cases mentioned above i.e. for ^{185}Bi. The most probable clusters in every region are shown and marked by deep minima's in potential. The general trend of the fragmentation is found to be similar in all the three cases.

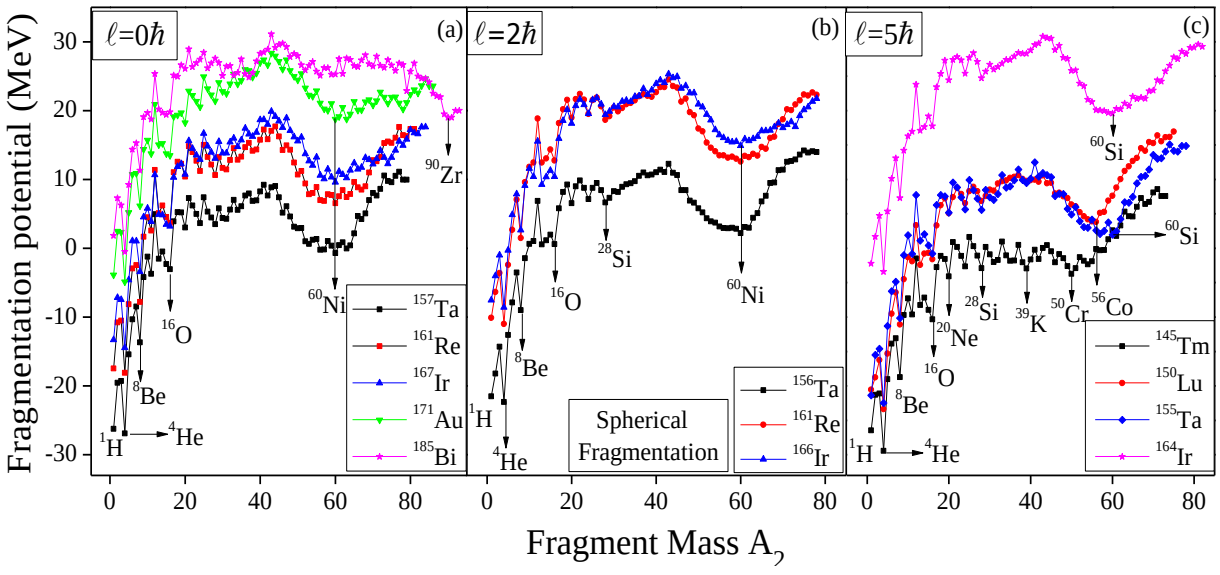

Figure 3.1: *Fragmentation potential as a function of fragment mass for different spherical proton emitters plotted for spherical fragmentation at (a) ℓ=0ħ (b) ℓ=2ħ (c) ℓ=5ħ.*

In case of ℓ=0ħ from panel (a), one can see that as we move towards the higher mass systems, the fission valley in fragment mass region 40-80 starts depleting but the most probable fragment in the fission region remains almost same except for the case of highest mass system i.e. ^{185}Bi. The overall distribution in fissioning region looks asymmetric except for ^{185}Bi. So, we can say that the existence of near-symmetric fission is dominant as we go towards higher mass systems. From panel (b), it is observed that although the potential energy surface (PES) remains similar for all the systems but magnitude of fragmentation potential is changing continuously. In fact, this behavior of potential is found in all the cases independent of its angular momentum value. Again for ℓ=2ħ case, the most probable fragment remains same for all the systems. In case of ℓ=5ħ, as we move from ^{145}Tm to ^{164}Ir, the distribution pattern still remains asymmetric and the potential dip in the fissioning region becomes sharper with the increase in mass of nucleus. Independent of inclusion of ℓ- effect, the fragmentation pattern in fissioning region appears to be symmetric, except for ^{185}Bi.The calculations of the decay constants and their corresponding half lives for all the systems have been done using PCM at different ℓ-values.

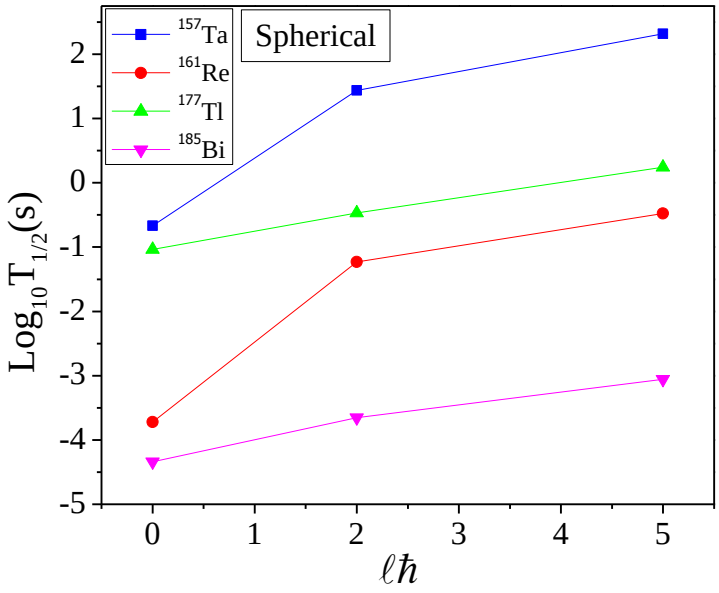

Figure 3.2: *Variation of half life values with different ℓ values for various spherical proton emitters.*

As stated in chapter 1, proton decay half lives are sensitive to ℓ-values. Figure 3.2 shows the change of logarithm of half lives with ℓ-values for four different proton emitters viz. ^{157}Ta,

^{161}Re, ^{177}Tl and ^{185}Bi. The neck length parameter *(ΔR)* is kept same at different ℓ-values for a system. From the figure, it is clear that the value of half life increases on increasing the angular momentum of the system. For heavier nuclei like ^{177}Tl and ^{185}Bi, the variation of half life is linear with ℓ-value but for comparatively lighter systems, the variation becomes non linear.

Since the preformed cluster decay model (PCM) has also been used for alpha decay studies in past [6], so we have compared the penetration path for proton decay vs. alpha decay of one of the spherical proton emitter i.e. ^{185}Bi. In figure 3.3, scattering potential is plotted as a function of range *R* that helps us to compare alpha decay dynamics and its penetration path with that of proton decay.

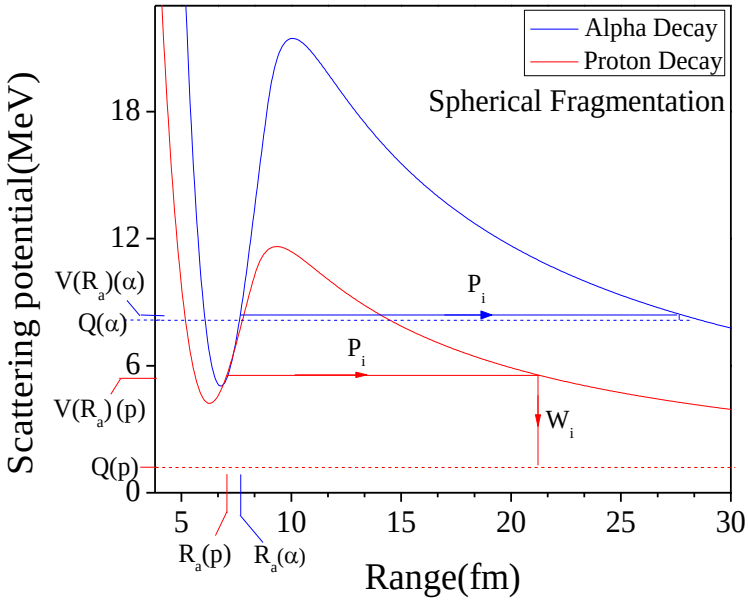

Figure 3.3: *Scattering potential as a function of range for both alpha and proton decay of spherical proton emitter ^{185}Bi.*

The graph is plotted for heaviest experimentally known spherical proton emitter ^{185}Bi. The above figure reveals that the potential barrier for alpha decay is higher than for the proton decay. The point R_a on the graph represents the first turning point i.e. tunneling of proton begins at $R=R_a$ and terminates at $R=R_b$ [7] (second turning point) with $V(R_b)=Q$ for ground state decay.

The potentials corresponding to R_a and R_b are represented by $V(R_a)$ and $V(R_b)$. The scattering potentials in Figure 3.3, plotted for the cases of proton and alpha decay, show that the barrier height as well as position get modified. In other words, barrier height gets reduced if we go to proton decay from alpha decay. Also, the turning points get changed accordingly. The potential corresponding to $V(R_a)(\alpha)$ is higher than that of $V(R_a)(p)$. So, proton decay is the preferable decay mode for ^{185}Bi than that of alpha decay as proton gets relatively easy path to penetrate the barrier.

Table 3.2: *Deformed proton emitters measured so far with experimental ℓ and $T_{1/2}$ values [10, 11, 12] and calculated values of P_0, P, half lives (calculated with old and new binding energies).*

Sr. No	Parent nuclei	ℓ ($\hbar$)	β_2	ΔR (fm)	Pref. Probability ($\log_{10} P_0$)	Penetrability ($\log_{10} P$)	$\text{Log}_{10}\ T_{1/2}$(s)		Q_p MeV
							Expt	Present	
1	^{109}I	2	0.160	0.05	-2.581	-14.970	-3.987	-3.966	0.821
2	^{112}Cs	2	0.208	0.62	-3.698	-14.528	-3.301	-3.284	0.812
3	^{113}Cs	2	0.207	0.44	-3.484	-13.302	-4.777	-4.762	0.974
4	^{117}La	2	0.290	1.15	-3.853	-16.057	-1.602	-1.597	0.822
5	^{121}Pr	2	0.318	1.12	-3.966	-15.551	-2.000	-2.002	0.892
6	^{130}Eu	2	0.331	0.09	-4.958	13.571	-3.046	-3.012	1.032
7	^{131}Eu	2	0.280	1.11	-4.139	-15.850	-1.575	-1.531	0.952
8	^{135}Tb	3	0.325	0.34	-3.511	-14.987	-3.027	-3.067	1.182
9	^{140}Ho	3	0.249	0.46	-4.772	-14.512	-2.222	-2.256	1.092
10	^{141}Ho	3	0.286	0.35	-3.790	-15.752	-2.387	-2.309	1.182

The another point of interest in ground state nuclear behavior is to address the role of deformations and orientations on decay half lives and other related parameters. Due to inclusion of deformations, the position and height of barrier get modified, so that the tunneling probability *P* get modified. The computed half-life $T_{1/2}$ depends on *P*, and hence on inclusion or non-inclusion of deformations and orientations of nuclei. Also, deformation effects play very significant role in the potential energy surfaces due to which the relative preformation probability P_0 gets modified. So, inclusion of deformation effects can provide significant influence on the study of decay characteristics. Our study is confined to quadrupole deformations (β_2) only and optimum orientations are used with cold elongated configuration [13].In present work, 10 cases of deformed proton emitters have been studied. Table 3.2 gives the detailed information of the several quantities such as preformation

probability P_0, penetrability P, decay half lives $T_{1/2}$, Q-values and the corresponding angular momentum values of the deformed proton emitters.

From the above table, a comparison can be made between experimental half lives and half lives calculated using PCM (using new binding energies). It is clear from the table that the calculated decay half lives are in a good agreement with experimental values. The half lives shown in the table are determined with the help of P_0 and P, P_0 depends explicitly on fragmentation potential. Fragmentation potential for the case of deformed system ^{109}I is plotted against fragment mass as shown in figure 3.4.

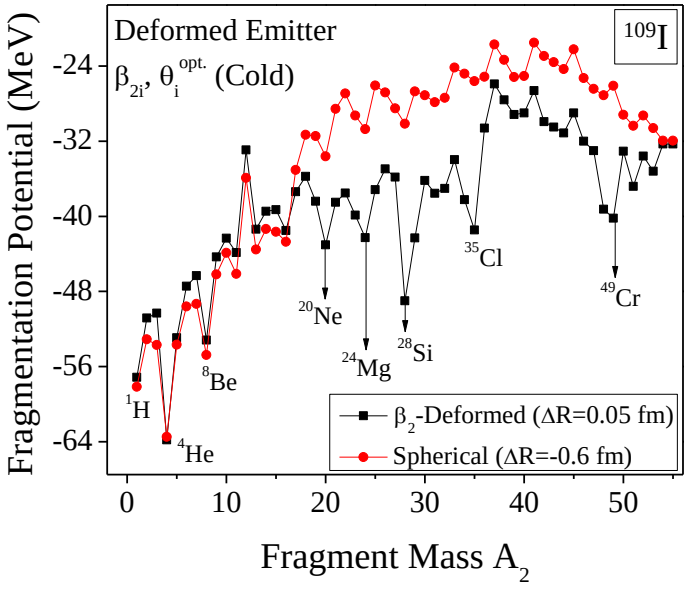

Figure 3.4: *Fragmentation potential as a function of fragment mass A_2 for deformed proton emitter ^{109}I using deformed as well as spherical choice of fragmentation.*

To examine the role of deformation, the above graph is plotted for ^{109}I (itself a deformed emitter) assuming spherical as well as deformed choice of fragmentation. From the above figure, it is noticed that for lower mass fragments the fragmentation potential for deformed choice is comparable with the spherical choice, whereas deformations play significant role for heavier mass fragments having A_2>16. One can see from the graph that although the potential energy surfaces (PES) pattern is almost similar for both the choices but the value of fragmentation potential increases considerably for higher mass fragments in case when decay fragments are considered as deformed. From the above fragmentation profile, it is also noted that mostly, α–like clusters are present on the deep minima's. Here also, for ^{109}I, there is a

possibility of alpha decay as the magnitude of fragmentation potential is significantly small independent of the choice of deformation effects.

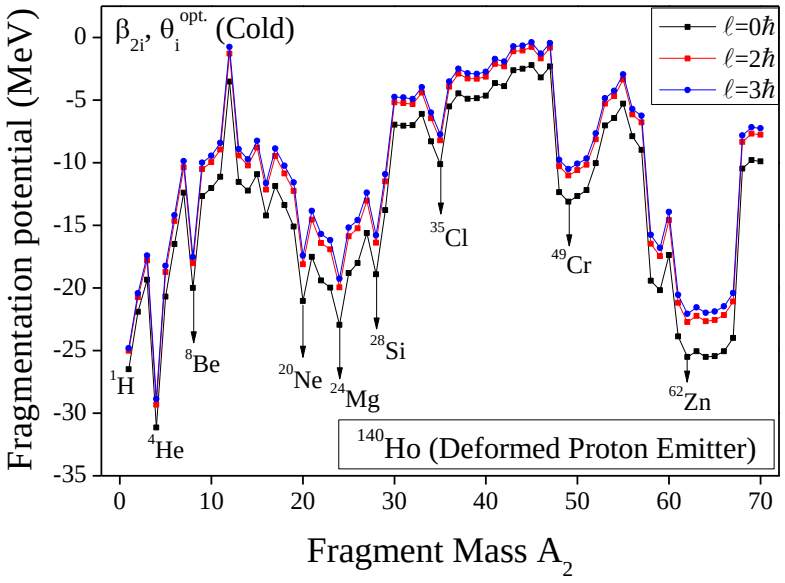

Figure 3.5: *Fragmentation potential plotted as a function of fragment mass A_2 for deformed proton emitter ^{140}Ho at different ℓ- values using deformed cold choice of fragmentation.*

To examine the effect of ℓ-value on proton decay, figure 3.5 is plotted to analyze the variation of fragmentation potential for ^{140}Ho nucleus, which is a deformed proton emitter. Besides the given experimental ℓ-value (ℓ=3ħ) for ^{140}Ho, we observed the fragmentation profile for ℓ=0ħ and 2ħ also. From the graph, it can be seen that as ℓ-value is increased, the magnitude of fragmentation potential gets enhanced. Also, it is noticed that the most probable clusters remain exactly same independent of the choice of angular momentum value. It is worth mentioning here that for ^{140}Ho, fission is the comparable decay mode with proton decay and the most dominant fission fragment is found to be ^{62}Zn at considered ℓ-value.

It is relevant to mention here that ΔR is the only parameter of the model which can be employed for best addressal of the experimental data. In figure 3.7, variation of ΔR and logarithm of half lives $T_{1/2}$ is plotted for different deformed proton emitters. It may be noted from the graph that the behavior of ΔR and $\log_{10}T_{1/2}$ is opposite to each. The pattern of the different emitters gets almost reversed. This observation seems to suggest that to get a shorter half life, larger value of neck is needed.

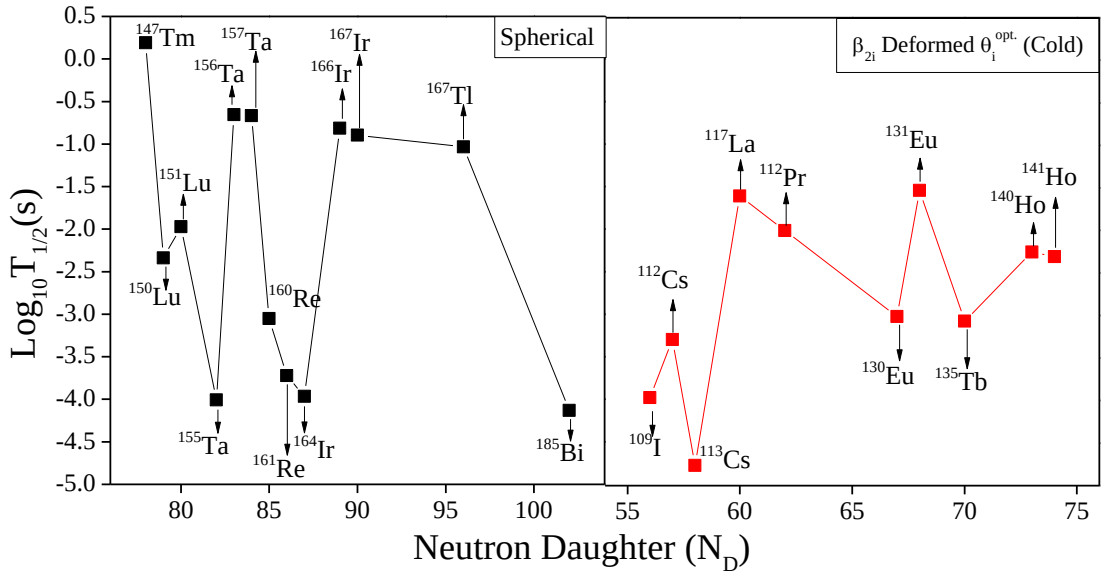

Figure 3.6: *The variation of half life of different proton emitters with number of neutrons in daughter nuclei (emitted by both spherical as well as deformed parent nuclei).*

Above figure shows the logarithm of proton decay half lives as a function of neutron number of daughter (N_D) nuclei emitted by various proton emitters. The $\log_{10}T_{1/2}$ (sec) values were found to be lowest for some neutron numbers which correspond to N=82, 87 and 102. The N=82 dip signifies the existence of spherical magic shell closure however further investigations are required to understand the existence of such dips at N=87 and 102. For deformed proton emitters, the $T_{1/2}$ dips are observed at N=58, 67 and 70, which are in close vicinity of observed deformed shell closures in this mass region[14]

The experimental and the half lives calculated half lives are shown in table 3.2. To analyze the deviation of calculated values from experimental data, figure 3.8 is plotted for the difference [$\log T_{1/2}$(Expt.) - $\log T_{1/2}$(PCM)] and case number (Sr. No. from table 3.2). The standard rms deviation from the experimental data for the deformed systems is also worked out.

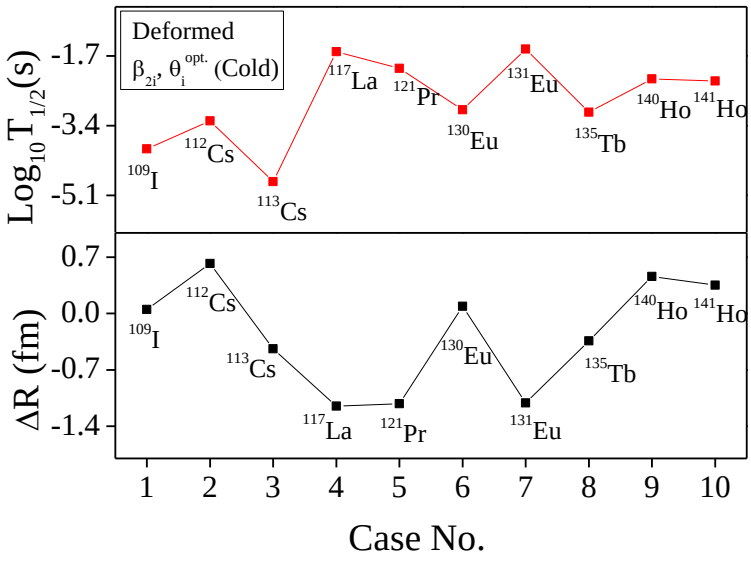

Figure 3.7: *Variation of neck length parameter ΔR and logarithm of half lives $T_{1/2}$ versus case no. for all the experimentally available deformed proton emitters using deformed choice of fragmentation having cold elongated configuration.*

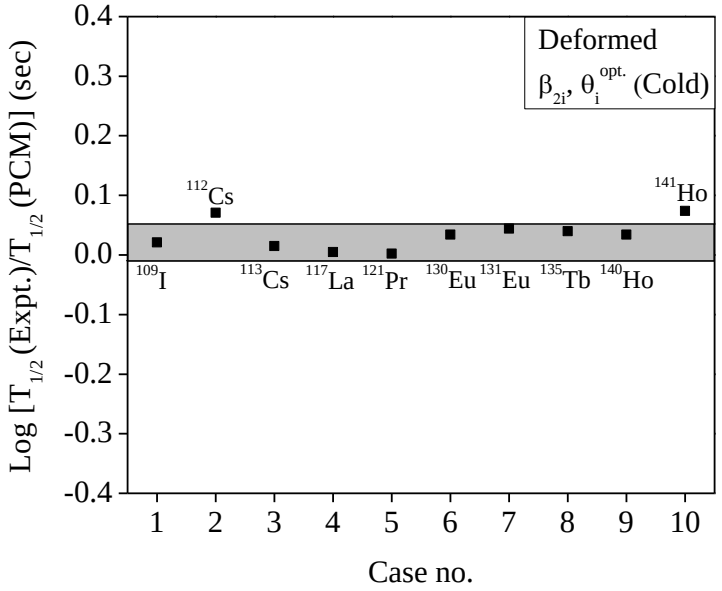

Figure 3.8: *Deviation of calculated half lives (PCM) from experimental values for deformed proton emitters.*

The deviation between the experimental values and those calculated by PCM is shown in figure 3.8. It clearly depicts that the values determined by PCM are in a nice agreement with

the experimental data except for the two cases. ^{112}Cs and ^{141}Ho have the deviation of approximately 0.08 sec from the experimental number. Rest of the nuclei give relatively better description of experimental data, within a range of -0.009 to 0.05 seconds. The standard rms deviation *(σ)* from the experimental data is also calculated for the above mentioned systems and is found to be 0.0435.

3.3 Summary

The phenomenon of disintegration of nucleus by emission of proton is known as proton radioactivity. The nuclei lying beyond the proton drip-line are proton rich and unbound for the proton emission; hence emit protons to become stable. The purpose of present work was to study the effect of deformations on the half lives of proton decay, besides analyzing the impact of new binding energies from AME (2012) on nuclear dynamics. In the present study, 14 cases of ground state (spherical) and 10 cases of ground state (deformed) nuclei were considered. It is shown that all the currently available experimental data available on these proton emitters can be interpreted within the framework of preformed cluster model (PCM) using latest data on binding energies and the calculated results are showing reasonably nice agreement with the available experimental data.

The relevant role of deformations of decaying fragments is also analysed in the fragmentation process of ^{109}I nucleus. It is observed that effect is significant for heavier decay products. The effect of angular momentum is seen for both deformed as well as spherical proton emitters. It is seen that on increasing the ℓ value, the magnitude of fragmentation potential increases. The trend of fragmentation profile seems to exhibit α-structuring pattern for both spherical and deformed proton emitters. The overall distribution of fragmentation potential for all the proton emitters looks asymmetric in fission region except for ^{185}Bi. Proton decay is also compared with alpha decay for heaviest parent nucleus ^{185}Bi. The penetrability pattern seems to suggest relatively easy path for the proton emission. Calculated values are compared with experimental ones and deviation of experimental half lives are also worked out. For deformed proton emitters, the deviation from the experimental numbers is in range -0.009 to +0.05 sec, except for ^{112}Cs and ^{114}Ho which have deviation of approximately 0.08 sec. The standard rms deviation for spherical and deformed proton emitters from their corresponding experimental data are found to be 1.231 and 0.0435 respectively.

This study seems useful to understand the decay properties and structure of proton rich nuclei, which exist near and beyond the proton drip-line. For the future purposes, new proton emitters can be deliberated through PCM. For comprehensive knowledge of fragmentation behavior of proton, alpha and cluster dynamics is important, and further analysis of related parameters can be worked out in near future. In other words, the scope of different decay modes such as alpha and cluster emission from the same proton emitters can be of future

interest and very relevant for better understanding of nuclear behavior near the proton dripline region .

3.4 References:

1. M. Wang, G. Audi, A.H. Wapstra, F.G. Kondev, M. MacCormick, X. Xu1, and B. Pfeiffer, Chin. Phys. C, 36, 12 (2012)
2. P.Moller, J.R Nix, W.D Myer and W.J Swiatecki, At. Data nucl. Data Tables 59, 185 (1995)
3. A. A. Sonzogni, Nuclear Data Sheets 95, 1 (2002).
4. A. H. Wapstra, G. Audi and C. Thibault, Nucl. Phys. A 729, 129 (2003)
5. R. Kumar, Phys. Rev. C 86, 044612 (2012).
6. Niyti, G. Sawhney, M. K Sharma, R. K Gupta, Phys. Rev. C 91, 054606 (2015).
7. S. K. Arun, R. K. Gupta, S.Kanwar, B.B Singh, M.K Sharma, Phys. C 80, 034317 (2009)
8. R. K. Gupta, Heavy Elements and Related New Phenomena, edited by W. Greiner and R. K. Gupta (World Scientific, Singapore, 1999), Vol. II, Ch. 18, p. 730.
9. S. S. Malik and R. K. Gupta, Phys. Rev. C 39, 1992 (1989).
10. A. A. Sonzogni, Nuclear Data Sheets 95, 1 (2002).
11. P. J. Woods et al., Phys. Rev. C 69, 051302(R) (2004).
12. A. P. Robinson et al., Phys. Rev. Lett. 95, 032502 (2005).
13. R. K. Gupta, M. Balasubramaniam, R. Kumar, N, Singh, M. Manhas, W. Greiner, J. Phys. G: Nucl. Part. Phys. 31, 631 (2005).
14. Y.T. Oganessian, R. Kalpakchieva, Nuclear physics shells-50 years, world scientific, Russia (1999)